Near IR diffraction-limited integral-field SINFONI spectroscopy of the Circinus galaxy

F. Mueller Sánchez, R. I. Davies, F. Eisenhauer,
L. J. Tacconi, and R. Genzel

*Max-Planck-Institut für extraterrestrische Physik, Postfach 1312, D-85741
Garching, Germany*

Abstract

Using the adaptive optics assisted near infrared integral field spectrometer SINFONI on the VLT, we have obtained observations of the Circinus galaxy on parsec scales. The morphologies of the H_2 (1-0) S(1) 2.12μm and Brγ 2.17μm emission lines are only slightly different, but their velocity maps are similar and show a gradient along the major axis of the galaxy, consistent with rotation. Since $V_{\rm rot}/\sigma \approx 1$ suggests that random motions are also important, it is likely that the lines arise in a rotating spheroid or thickened disk around the AGN. Comparing the Brγ flux to the stellar continuum indicates that the star formation in this region began $\sim 10^8$ yr ago. We also detect the [SiVI] 1.96μm, [AlIX] 2.04μm and [CaVIII] 2.32μm coronal lines. In all cases we observe a broad blue wing, indicating the presence of two or more components in the coronal line region. A correlation between the ionisation potential and the asymmetry of the profiles was found for these high excitation species.

Key words: Integral Field Spectroscopy; SINFONI; Active galaxies; Circinus; starburst

1 Introduction

The star formation history, the mass distribution, and the stellar and gas dynamics on scales of less than a few parsecs in the nuclei of Seyfert galaxies, are some of the main debated issues in the context of active galactic nuclei. The Circinus galaxy, at a distance of 4.2 ± 0.8 Mpc (Freeman et al. (1977)), is an ideal subject to study because of its proximity ($1'' = 20$ pc). It is a large, highly inclined ($i = 65°$), spiral galaxy that hosts both a typical Seyfert 2 nucleus and a circumnuclear starburst. This work comprises a summary of the results obtained after analyzing the SINFONI datacube of the Circinus galaxy presented in Mueller Sánchez et al. (2006)

2 The instrument: SINFONI

SINFONI comprises an Adaptive Optics facility (AO-Module), developed by ESO (Bonnet et al. (2003)) and SPIFFI, a NIR integral field spectrograph developed by MPE (Eisenhauer et al. (2003)). The AO-Module consists of an optical relay from the telescope's Cassegrain focus to the SPIFFI entrance focal plane, which includes a deformable mirror conjugated to the telescope pupil. The curvature is updated on the 60 actuators at 420 Hz, with a closed-loop bandwidth of 30–60 Hz, to compensate for the aberrations produced by the turbulent atmosphere. Under good atmospheric conditions an adequate correction can be obtained over the full 1×2 arcmin^2 FOV with stars up to $R = 17$ mag. The SPIFFI integral field spectrometer records simultaneously the spectra of all image points in a two-dimensional field of view. The image scale of SPIFFI allows sampled imaging at the diffraction limit of the telescope $(0.0125''/\text{pix})$, seeing limited observations $(0.125''/\text{pix})$ and an intermediate image scale $(0.05''/\text{pix})$, over a FOV of $0.8'' \times 0.8''$, $8'' \times 8''$, and $3.2'' \times 3.2''$ respectively. The spectral resolution of the spectrometer ranges between 2000-5000 for the three covered atmospheric bands: J $(1.1\mu\text{m}–1.4\mu\text{m})$, H $(1.45\mu\text{m}–1.85\mu\text{m})$ and K $(1.95\mu\text{m}–2.45\mu\text{m})$. The instrument is fully cryogenic, and it is equipped with a Rockwell 2k×2k HAWAII-2RG array. Figure 1 shows an inside view of the main components of SPIFFI. The light enters from the top. The pre-optics with a filter wheel re-image the object plane from the AO module onto the image slicer, providing the three different image scales. The image slicer rearranges the two dimensional field onto a one-dimensional pseudo longslit. A grating wheel disperses the light and a short focal length camera then images the spectra on the detector. After some processing of the raw data, the outcome is a data cube with two spatial and one spectral dimensions.

3 Nuclear dust emission

Images of the $2\mu\text{m}$ continuum and the Brγ and H$_2$ (1-0) S(1) line emission, as well as the ^{12}CO (2-0) band flux are presented in Figure 2. The SINFONI PSF was found to be wll represented by a symmetrical moffat function, with a FWHM spatial resolution of $0.2''$.

In Circinus, although the AGN is highly obscured, it is revealed indirectly by the compact K-band non-stellar core. The fraction of stellar light in the nucleus is deduced from comparison of the $EW(^{12}\text{CO} (2-0))$ absorption bandhead with star clusters models. The intrinsic equivalent width is pretty much independent of star formation history for an ensemble of stars as predicted by the models, and it has an almost constant value of ~ 12Å (Davies et al.
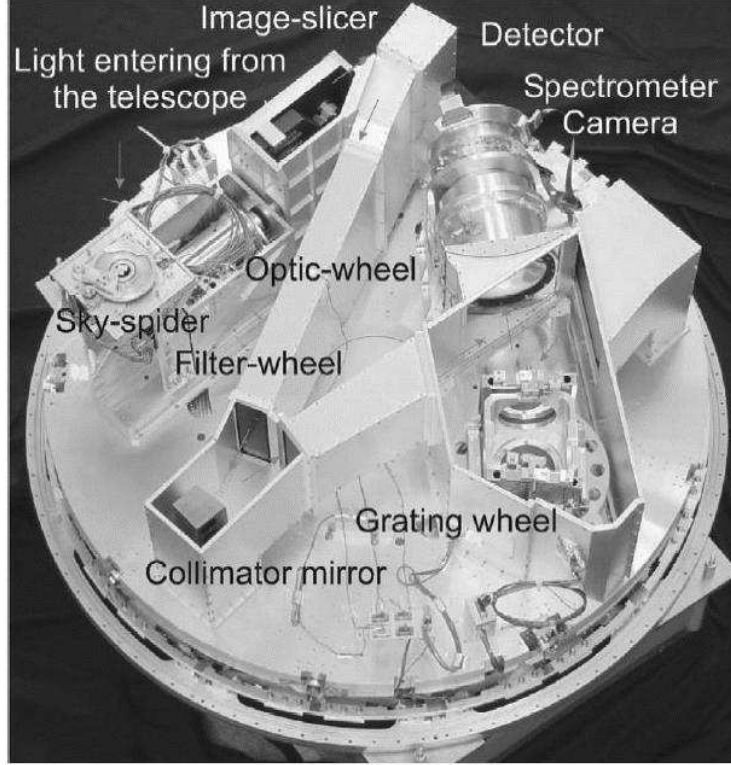
Fig. 1. An inside view of SPIFFI (Read text for the explanation)

(2006)). The stellar continuum, which accounts for only $\sim 15\%$ of the total K-band luminosity in the central arcsec, shows a much broader distribution than the non-stellar part. This extended morphology is also reflected in the H_2 (1-0) S(1) and $Br\gamma$ line profiles. On these scales, less than 20 pc, an exponential profile with $r_d = 4^{+0.5}_{-0.1}$ is an excellent match for each of the lines, consistent with the hypothesis that the stars and the molecular gas reside in a thickened disk or rotating spheroid, as suggested by the kinematics (see Section 4).

We have partially resolved the non-stellar K-band source. A quadrature correction of its FWHM with that of the PSF yields an intrinsic size of ~ 2 pc, consistent with that found by Prieto et al. (2004) and also with the sizes predicted by the unification model, in which the hot dust (~ 1000 K) lies ~ 1 pc away from the AGN.

4 Star formation activity and gas kinematics

As the AGN is highly obscured, no broad line region is visible. This, together with the symmetry of the narrow line emission and its uniform velocity field, suggests that the $Br\gamma$ emission is associated with star formation activity surrounding the Seyfert nucleus. This picture is supported by the similar
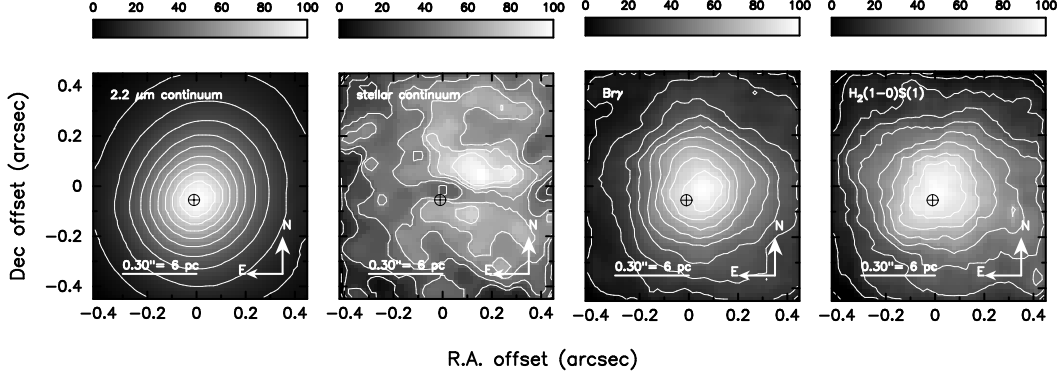
3

Fig. 2. Intensity images extracted from the SINFONI data cube in the central arcsec of Circinus. In each case, the gray scale extends from 0-100% of the peak flux, and contours are spaced equally between 20% and 90% of the peak flux. An encircled cross indicates in each case the peak of the continuum emission. The maps show, from left to right: 2.2μm continuum, stellar continuum (derived from the stellar absorption bandhead ^{12}CO(2-0)), Brγ, and H_2(1-0)S(1).
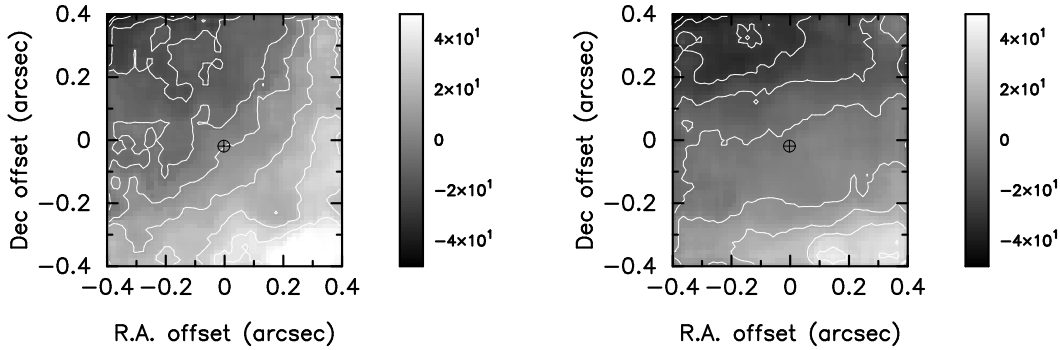

Fig. 3. Velocity maps of the central $0.8'' \times 0.8''$ of Circinus. In each case, the gray scale extends from [-50, 50] km s^{-1}, and contours are spaced equally every 10 km s^{-1}. An encircled cross indicates in each case the peak of the continuum emission. The maps show, *Left*: H_2(1-0)S(1). *Right*: Brγ

morphologies in the Brγ, ^{12}CO (2-0) and H_2 maps, and the consistency of the velocity fields and dispersion maps of the Brγ with the H_2. By comparing the evolution of the $EW(\text{Br}\gamma)$ and ν_{SN}/L_K^* with time, a moderate duration of the star formation $t_{scl} = 10^8$ yr, and an age of 8×10^7 yr fit best our observational constrains of $EW(\text{Br}\gamma) = 30$ Å and $\nu_{SN}/L_K^* = 1.47 \times 10^{-10}$ $L_\odot^{-1}$ yr^{-1}, indicating the presence of a young stellar population within a few parsecs ($R < 8$ pc) of the active nucleus.

The projected velocity maps of the H_2 (1-0) S(1) and the Brγ lines show a velocity gradient consistent with simple rotation with the same major axis as the large scale galaxy as can be seen in Figure 3. By correcting the velocity maps for inclination ($i = 65°$), a rotation velocity of 75 km s^{-1} at 8 pc from the nucleus was found. The intrinsic velocity dispersion of the stars in the nuclear region is almost constant with a value of ~ 70 km s^{-1}. Using these values we
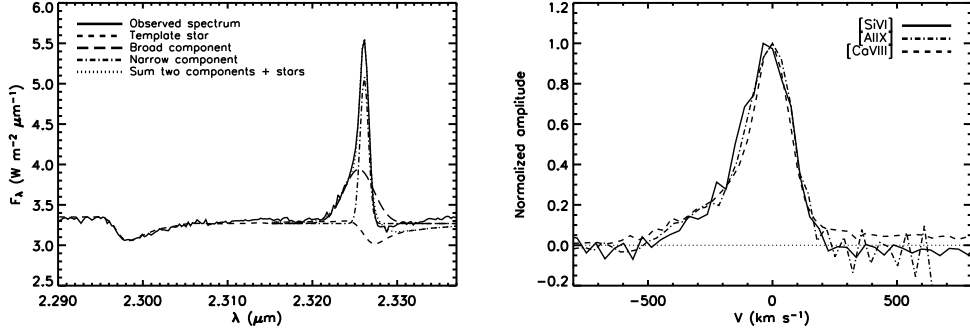
Fig. 4. *Left panel:* Nuclear spectrum around [CaVIII] showing how the stellar continuum was substracted and the two components forming the line profile. *Right panel:* Comparison of coronal line profiles in velocity space.

obtained an intrinsic velocity to dispersion ratio in the maps of $V_{\rm rot}/\sigma \approx 1.1$ Because this ratio is ~ 1, it is an indication that, in addition to rotation, random motions are also significant in the nuclear region.

5 The coronal lines

In our observations of Circinus the highly ionised [SiVI], [CaVIII] and [AlIX] emission lines are detected. In all three profiles we observe asymmetric and broadened lines, indicating the presence of two or more components inside the coronal line region. Indeed, the three asymmetric coronal lines were best fitted by the superposition of two Gaussians as can be seen in Figure 4 for the case of the [CaVIII] emission line. The kinematics of the coronal gas were also analyzed by comparing the emission line profiles of the three coronal lines. Figure 4 also shows the results for the three high excitation lines detected with SINFONI. The blue shifted (-100 to $-200\,\mathrm{km\,s^{-1}}$) broad ($>300\,\mathrm{km\,s^{-1}}$) wing is spatially extended. On the other hand, the narrow component is at systemic velocity and spatially compact. These characteristics suggest that the two components originate in different regions and could even be excited by different mechanisms. In the case of the broad component, its blue shift indicates that part of the gas must arise in outflows around the AGN (Rodríguez-Ardilla et al. (2004)). The most likely scenario is that this comprises a multitude of outflowing cloudlets producing many narrow components at different velocities which combine to produce the observed morphology and profile. It has been suggested that similar out-flowing cloudlets in NGC 1068 might arise from ablation of the larger clouds (Cecil et al. (2002)). In the case of the narrow component, the fact that it is compact, centered on the nucleus, and at the systemic velocity suggest that it originates physically close to the AGN. The narrow line width ($\sim 180\,\mathrm{km\,s^{-1}}$) indicates that they must be excited by photoionization from a hard ionising continuum (Oliva (1999)).

Interestingly, we observe correlations between the ionisation potential (IP) and both the blueshift and relative strength of the broad wing, indicating that different species (with different IP) originate in different regions. We suggest that the higher ionization species have faster outflow velocities because they are closer to the AGN where the radiative acceleration is stronger (and the cloudlets have not been slowed by travelling a long distance through the interstellar medium), and weaker fluxes because there are fewer photons hard enough to ionise them.

References

[2003] Bonnet, H., et al. 2003, SPIE, 4839, 329

[2002] Cecil, G.,Dopita, M. A., Groves, B., Wilson, A. S., Ferruit, P., Pécontal, E., Binette, L. 2002, ApJ, 568, 627

[2006] Davies, R. I., et al. 2006 in preparation

[1977] Freeman, K. C., Karlsson, B., Lyngå, G.,Burrell, J. F., van Woerden, H., Goss, W. M., Mebold, U. 1977, A&A, 55, 445

[2003] Eisenhauer, F. et al. 2003, SPIE, 4844, 1548

[2006] Mueller Sánchez, F., et al. 2006 in preparation

[1999] Oliva, E., Marconi, A., Moorwood, A. F. M. 1999, A&A, 342, 87

[2004] Prieto A., Meisenheimer, K., Marco, O., et al. 2004, ApJ, 614, 135

[2004] Rodríguez-Ardilla A., Pastoriza, M., Viegas, S., Sigut, T., Pradhan, A. 2004, A&A, 425, 457